Article

Syngas from waste plastics and water using Joule heating

Check for updates

Qing Ma[1], Yongjun Gao ®[1] ✉, Chengcheng Cai ®[2], Tianfu Wang ®[2] ✉ & Ding Ma ®[3] ✉

The development of innovative, sustainable, and atom-economic methods to tackle the escalating problem of plastic pollution is crucial. A Joule-heating system capable of reforming waste plastics and water into syngas has been developed, which can process 2.5 g of waste plastic (equivalent to a whole plastic food bag) and 5.5 g through ten batches of reaction. Control experiments, kinetics, and in-situ experiments reveal that the proton hopping under the electric field is the key step in reforming gaseous hydrocarbons with water into syngas. Due to its high energy efficiency, this wet reforming system can utilize solar energy as the sole energy source, extracting syngas from waste plastic and water without the need for additional transition metal catalysts. Consequently, this approach offers an efficient strategy for storing solar energy in the form of syngas and offers a sustainable solution to the environmental challenges posed by the accumulation of plastic waste.

Syngas, a mixture of carbon monoxide (CO) and hydrogen (H_2), is a crucial intermediate for the production of bulk chemicals such as methanol and synthetic fuels[1]. Current syngas production methods predominantly rely on fossil-based feedstocks, including coal, natural gas, and heavy oil. These processes are energy-intensive and contribute significantly to greenhouse gas (GHG) emissions[2]. Thus, substituting fossil raw materials and fuels in the syngas production process can reduce dependence on fossil resources and potentially decrease or eliminate GHG emissions.

Plastics, collectively known as synthetic polymers, are primarily derived from fossil resources and are indispensable in modern life[3–6]. Global plastic production exceeds 430 million tons annually, with nearly two-thirds destined for short-lived applications. Following their brief utility, these plastics contribute to vast accumulations of waste, posing threats to ecosystems and human health[7,8]. Traditional disposal methods, such as landfilling and incineration, come with significant drawbacks, including farmland contamination and high CO_2 emissions. This highlights an urgent need for environmentally friendly and sustainable strategies to manage plastic waste[9–12]. Currently, various chemical methods have been developed to upcycle or depolymerize

waste plastics with the assistance of various catalyst[13]. Catalytic pyrolysis, hydrogenolysis, and alcoholysis can all transfer various plastics into high-value chemicals[14–19]. Furthermore, the high CH_2 content of plastics makes them an attractive alternative to fossil feedstocks for syngas production[20,21]. Two-stage strategies have been developed, wherein plastics are first gasified into gaseous hydrocarbons and then reformed with CO_2 or H_2O at elevated temperature to produce syngas[22–24]. However, the high temperature required in these processes typically depends on fossil fuel combustion, which consumes resources and releases CO_2. Plasma catalysis can provide high temperatures for the reforming process and achieve an ideal yield of syngas. Nevertheless, this approach necessitates specialized equipment, including ultrahigh-frequency high-voltage generators and high-melting-point electrodes/catalysts. Moreover, even state-of-the-art plasma-catalytic systems for plastic reforming still require energy-intensive pre-gasification steps, limiting their sustainability. To enhance the sustainability of waste plastics processing, renewable energy sources, such as solar energy and wind energy, have been adopted directly or indirectly[25]. For instance, photothermal systems powered by sunlight can convert mixed waste plastics containing

[1]Hebei Research Center of the Basic Discipline of Synthetic Chemistry, College of Chemistry and Materials Science, Hebei University, Baoding, China. [2]School of Environmental Science and Engineering, Frontiers Science Center for Transformative Molecules, Shanghai Jiao Tong University, Shanghai, China. [3]Beijing National Laboratory for Molecular Sciences, New Cornerstone Science Laboratory, College of Chemistry and Molecular Engineering, Peking University, Beijing, China. ✉e-mail: yjgao@hbu.edu.cn; tfwang@sjtu.edu.cn; dma@pku.edu.cn

polyvinyl chloride into methane and hydrochloric acid, with the required hydrogen supplied by a photovoltaic-powered electrolyzer. Similarly, Joule heating systems coupled with photovoltaics have been used to reform plastics with CO_2 into syngas[26]. However, a small amount of char and tar was left in the system, resulting in the low carbon utilization in waste plastics, especially in the large-scale reactor. In addition, the real waste plastics are not clean and usually contain various contaminants, such as food residues, oil, and dyes, which makes it difficult for the developed catalytic systems to upcycle real waste plastics directly. Therefore, it needs to further develop an excellent catalytic system to transform real waste plastics into value-added chemicals.

Herein, a wet reforming system promoted by Joule heating was developed to convert various waste plastics, including food residues, vegetable oil, and water, into syngas. The electrified FeCrAl heating wire in the center of the reactor provides the high temperature for instant gasification of plastics and water, as well as active catalytic sites to reform gaseous hydrocarbons and steam into syngas. Water in the system provides hydrogen and oxygen elements to reform the framework of plastics into CO and H_2. The presence of excess water does not generate further CO_2 in the system, making the reforming system suitable for converting the real waste plastics containing food residues, oil, and even wastewater into syngas. The scaled-up reactor is capable of processing 0.25 g of waste polyethylene (PE) plastic and 0.55 g of water within 25 min, and can be recycled at least ten times, totally converting a total of 2.5 g of waste plastic (equivalent to a whole plastic food bag) and 5.5 g of water into syngas. By using a photovoltaic system under sunlight to electrify the heating wire, the large-scale wet reforming process can be carried out smoothly. This work presents a practical and efficient approach for addressing plastic pollution by using solar energy to extract carbon/hydrogen resources from waste plastic and water without the need for precious metal catalysts.

Results

Wet reforming of plastics

In general, instruments for the reforming of plastic with CO_2 or H_2O typically consist of two furnaces[27]. The first furnace is used to pre-pyrolyze plastic into gaseous hydrocarbons, while the second furnace reforms these hydrocarbons with H_2O or CO_2 to produce syngas. The active reforming catalyst and high temperature in the second furnace are essential to the reforming process[28]. In addition, residual carbon is inevitably generated in the pre-pyrolysis furnace, which leads to the waste of the carbon source in plastics. Moreover, the energy utilization efficiency of the two-segment instrument is suboptimal due to heat conduction losses from the furnace to the reactant or catalyst bed. Joule heating reactor is an internal heating reactor that avoids the heat conduction process, thus leading to high energy utilization efficiency[29]. Additionally, the instantaneous heating feature of Joule heating minimizes some side reactions during plastic gasification. To facilitate the feeding of plastics into the Joule heating zone, a T-type quartz or stainless-steel reactor equipped with two electrodes, two ball valves, one inlet, and a heating wire was developed (Fig. 1).

In the initial stage screening and optimizing reaction conditions, the reactor was composed of a T-type quartz tube, two sets of metal flange equipped with a ball valve and an electrode, and a metal blind flange as reactant inlet (Supplementary Fig. 1, the detailed information was presented in the part of Methods. Warning: experimental operator must take personal protective equipment). The T-type quartz tube has the following dimensions: a main tube length of 100 mm, a side arm length of 50 mm, an outer diameter of 25 mm, and an inner diameter of 19 mm. Therefore, the thickness of the quartz tube wall is 3 mm, which can tolerate moderate pressure during the experiment. In this study, the product yields are calculated relative to the elemental content of the plastic reactant as the theoretical yield, enabling direct evaluation of elemental recovery efficiency from plastic feedstock. Consequently, in the PE wet reforming reaction, the theoretical H_2 yield may exceed 100% when the CO yield surpasses 50%. The contribution of water to hydrogen production can be quantified through either the CO yield or the difference between H_2 and CO yields (H_2 yield−CO yield). When using 14 mg PE powder (which can be considered as 1 mmol CH_2) as a model plastic reactant, it requires at least 1 mmol H_2O to convert into H_2 and CO. Therefore, 14 mg PE and 20 μL H_2O were initially added to the Joule heating reactor. As a heating component, a length of heating wire (2 Ω) was installed in the reactor, and a current of 7 amperes flowed through the heating wire. The temperature in the reactor can instantly reach 800 °C. After 12 min, 0.70 mmol CO and 1.22 mmol H_2 can be obtained, which corresponds to the H_2 and CO yields of 122% and 69%. In addition, 0.003 g residual carbon and trace amounts of
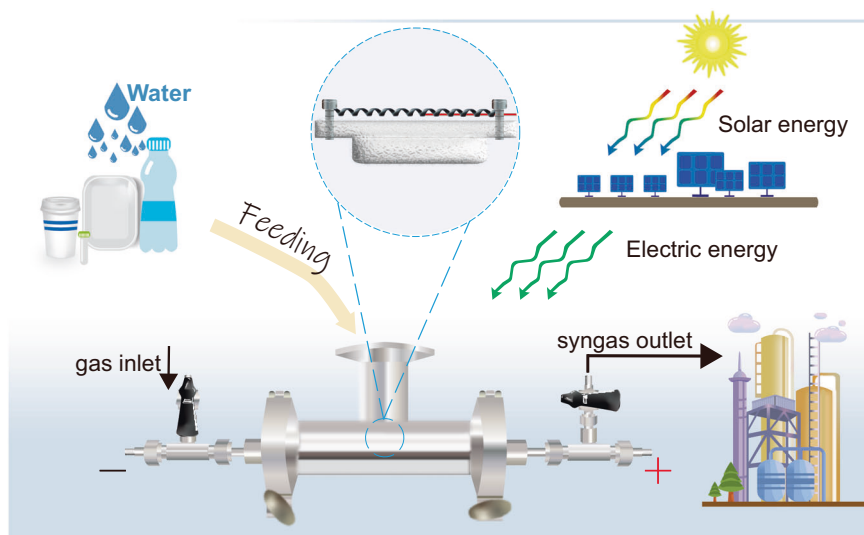

Fig. 1 | Schematic diagram of the Joule heating-promoted wet reforming of waste plastics using solar energy. A Joule heating system powered by solar energy for reforming waste plastics and water into syngas.
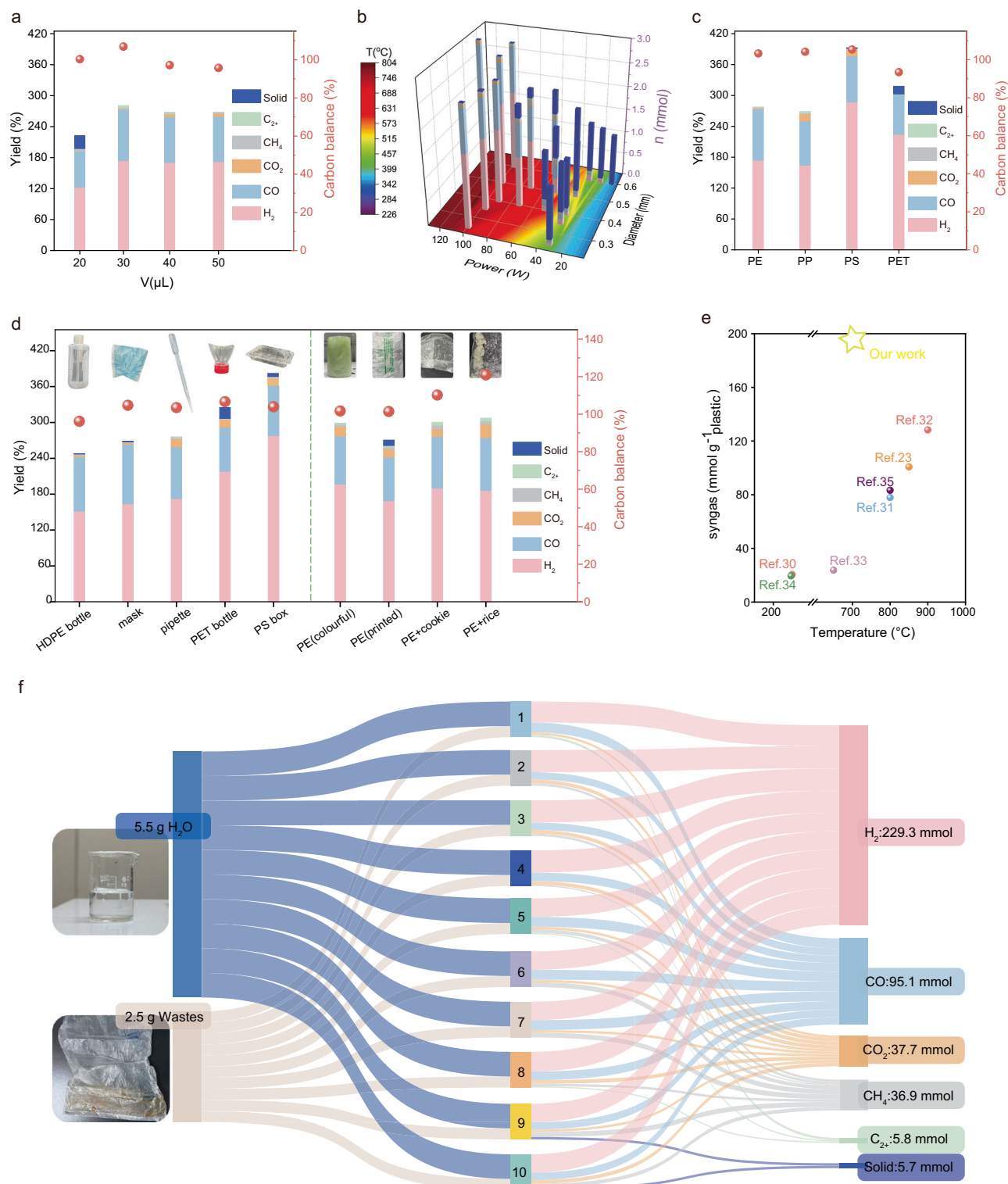
Fig. 2 | Reforming performance over FeCrAl wire and the comparison with other systems. a PE wet reforming with different H_2O quantity, Reaction conditions: PE 14 mg, FeCrAl heating wire 2 Ω, current 7 A,12 min; **b** screening of electrified power and heating wire diameters, Reaction conditions: PE 14 mg, H_2O 30 μL, 12 min; **c** wet reforming of various plastics, Reaction conditions: n(CHx) 1 mmol, FeCrAl heating wire 2 Ω, current 7 A; **d** wet reforming of various plastic product and PE bag containing colorants, paint and food residue. **e** The comparison of the current work with other reported reports and **f** wet reforming results of a real PE bag in a ten-continuous reforming process. Reaction condition for each batch: PE bag 0.25 g, H_2O 550 μL, FeCrAl heating wire 4 Ω, current 7 A, 25 min.

CO_2 were detected, with the carbon balance reaching almost 100% (Fig. 2a). The detailed calculation for carbon balance is presented in the Supplementary Tables 1–3. To fully utilize the carbon elements in PE, excessive amounts of H_2O should be added. In the presence of 30 μL H_2O, 0.99 mmol CO and 1.74 mmol H_2 can be obtained, which is close to the theoretical yields and achieves an ideal carbon balance. The yields of H_2 and CO reach 174% and 99%, respectively. When the amount of H_2O was further increased to 50 μL, 0.063 mmol CO_2 was detected, corresponding to a decrease of CO yield from 0.99 mmol to 0.89 mmol, and a maintenance of the H_2 yield at approximately 172%.

This indicates that a small amount of water reacted with CO to produce CO_2 and H_2 even in the presence of excess H_2O, further demonstrating the high selectivity of the reforming system to syngas. Ultimately, 30 μL was selected as the optimal dosage for reforming 1 mmol of CH_2 in plastics to syngas in the subsequent research. In addition, the heating wire in the Joule heating reactor is a key component for providing the high temperature. The diameter of the heating wire determines the resistance value per unit length and its tolerance to the maximum current (Supplementary Fig. 2 and Supplementary Table 4). The thinner heating wire has a higher resistance value per unit length, but a lower tolerable maximum current. The thicker one has a smaller resistance value per unit length but a larger tolerable current. When the resistance value of the heating wire was set at 2 Ω across different diameters and the maximum tolerable current was applied, the reforming performance varied with the heating wire diameter. It was found that the syngas yield was proportional to the power of the heating wire (Fig. 2b). When the power was kept at 100 W for each heating wire with different diameter and the maximum tolerable currents were selected (the length and resistance value are different for different heating wires), the syngas productions on different electrified heating wires were almost the same (Fig. 2b). However, if the current flow through the heating wire was not large enough to keep the heating wire in a red-hot state, the syngas yield was not ideal despite a power of 100 W. These findings indicate that both the power and the maximum working current of the heating wire are key factors that affect the reforming performance. Specifically, the heating wire should be in a glowing state and have enough power to reach a high temperature in the reactor and thus promote the reforming of PE and water into H_2 and CO.

More importantly, other plastics, such as polypropylene (PP), polystyrene (PS) and polyethylene terephthalate (PET) can also be reformed into syngas with water within 12 min (Fig. 2c). Due to the 1:1 carbon-to-hydrogen (C/H) ratio in PS, water contributes more significantly to hydrogen production in PS wet reforming compared to PE, achieving 287% of H_2 yield. Furthermore, higher CO_2 yields were observed in PP and PS reforming compared to PE wet reforming, likely attributable to their higher C/H ratios. For PET with C/H/O of 10:8:4, a tiny amount of solid was left after the wet reforming reaction. These results demonstrate that the composition or molecular structure of plastic influences the reforming performance, suggesting different reforming mechanisms for different plastics. The reforming mechanisms for different plastics will be researched in the part of Mechanism research. To demonstrate the practical application in upcycling waste plastics, the real plastic items, such as high-density polyethylene (HDPE) bottle, surgical mask, PE pipette, PET bottle, PS box, colored PE bag and printed PE bag can all be reformed with water to produce syngas (Fig. 2d). Notably, the Joule-heating promoted wet reforming system can convert actual plastic waste contaminated with food residues (rice/cookie crumbs) into syngas. The carbon balance exceeding 100% indicates that both the PE bag and carbohydrate components (food residues) can be reformed with water under optimal reaction conditions. Under optimal conditions, the syngas production performance of the Joule heating system is promising compared to other reforming systems (Fig. 2e and Supplementary Table 5)[23,30–35]. In addition, the system does not require special catalysts and does not generate solid residues, making it easier to operate and scale up. Therefore, the waste plastics collected in the rubbish dump can be reformed into syngas directly or after simple cleaning with water. The water remaining in the waste plastics can directly serve as a reactant in the reforming of waste plastics. To demonstrate the practical application in converting plastic waste, a custom-fabricated T-type stainless-steel reactor was developed, which has an inner diameter of 35 mm, an outer diameter of 38 mm, and a main tube length of 125 mm, which houses a quartz boat equipped with a heating wire at its center. The side tube is 43 mm long and serves as the feeding inlet. For safety, a pressure gauge and a decompression valve are equipped (Supplementary Fig. 3). In this stainless-steel reactor, 0.25 g of PE and 0.55 mL of water were reformed into syngas in 25 min in each batch reaction. As shown in Figs. 2f, 2.5 g of real waste plastic and 5.5 g of water were converted into approximately 229 mmol H_2 and 95 mmol of CO over ten batch reactions under laboratory conditions, achieving an ideal carbon balance (Supplementary Tables 6 and 7). This demonstrates the practical applicability of the Joule heating reforming system for upcycling waste plastics and extracting hydrogen from water. This technology, therefore, offers a viable alternative to electrochemical hydrogen production, eliminating the need for noble metal catalysts.

Notably, trace amounts of residual solid and C_{2+} hydrocarbons were detected during the final two cycles of the ten recycling experiments, concomitant with an increase in CH_4 yields. This observation suggests that the accumulation of residual coke adversely affected the wet reforming of PE under the optimal reaction conditions. To validate this hypothesis, 0.5 mg of coke derived from PE dehydrogenation was introduced into the PE wet reforming system. If the water dosage was still same to the one in optimal conditions, more CO_2 and hydrocarbons were detected and more solid was left (Supplementary Fig. 4). We deduced that the coke in the system consumed some water to produce H_2 and CO_2 so that the water in the system is not enough to reform the PE. If 90 μL of water was introduced into the system, the yields of H_2, CO_2, and CO all increased, although a small amount of solid was still left, accompanied by a carbon balance of 120%. Thus, it can be concluded that the coke accumulated in the system competitively consumed water, impacting the PE wet reforming performance. However, this adverse factor can be eliminated or reversed by increasing the water dosage in the wet reforming reaction.

Mechanism research

To investigate the reforming mechanism of plastic over electrified heating wire, the kinetics of various experiments, such as wet reforming of PE, PE dehydrogenation, and water decomposition, were carried out over electrified heating wire. Under optimal conditions, the residual solid gradually decreased with the increasing reaction time, corresponding to the simultaneous increase in CO and H_2 yields (Fig. 3a). A small amount of coke deposited on the boat was observed at the initial stage of the reaction, and was eventually reformed into CO in the presence of H_2O finally (Supplementary Fig. 5). The yield of CH_4 peaked in the first half of the reaction time, indicating its role as an intermediate in the reforming process. When no water was present in the reactor, PE dehydrogenation occurred (Fig. 3b). The residual mass in the system initially decreased before increasing as the reaction progressed, which correlated with an initial rise and subsequent decline in hydrocarbon yields (CH_4 and C_{2+}). The H_2 yield increased rapidly in the initial stage, then slowly until the reaction was completed. These results suggest that PE dehydrogenation and decomposition both occurred at the initial stage when there was no water in the reaction system, resulting in a residual decrease. With the dehydrogenation of the gaseous hydrocarbons, the H_2 yield and the residual mass increased gradually in the last half of the reaction stage. The morphology of coke generated from PE dehydrogenation resembles that generated at 3 min during the wet reforming of PE (Supplementary Fig. 6), with both exhibiting aggregated nanospheres. The H_2 production in PE wet reforming is higher than that in PE dehydrogenation at any time point, showing the important contribution of water decomposition to H_2 production.

Based on the comprehensive kinetic data, it has been determined that the degradation pathways of PE, whether through wet reforming or dehydrogenation processes, consistently exhibit first-order reaction behavior, as evidenced by the linear relationship between $\ln(1/a)$ and reaction time (Fig. 3c). The letter "a" in $\ln(1/a)$ represents the mole number of PE left in the reactor at each reaction time "t". The rate constant of PE degradation in wet reforming of PE is about
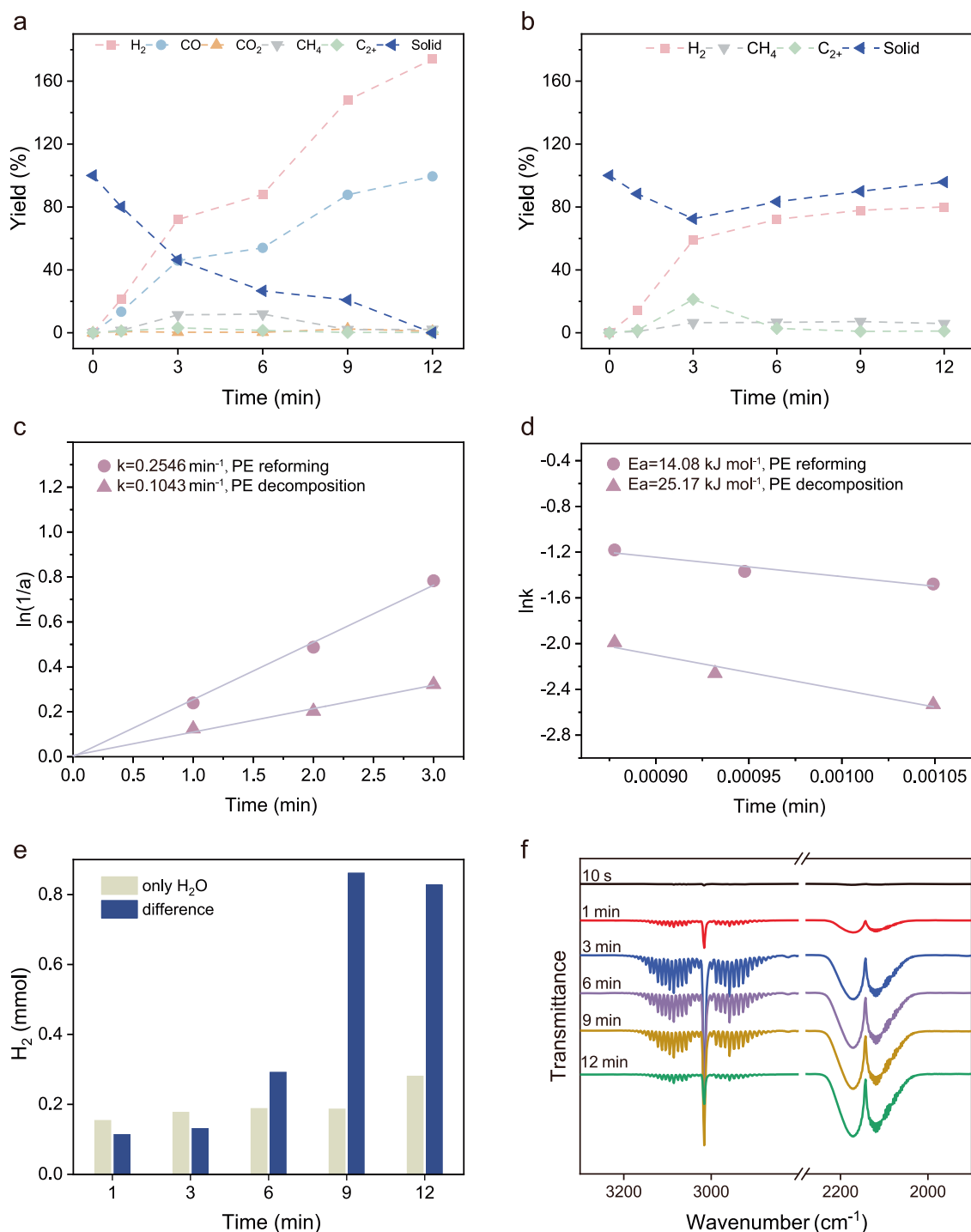
Fig. 3 | Kinetic studies of the wet reforming and dehydrogenation of PE.
a Kinetics of wet reforming of PE, Reaction conditions: PE 14 mg, H_2O 30 μL, FeCrAl heating wire 2 Ω, current 7 A; **b** kinetics of PE decomposition, Reaction conditions: PE 14 mg, FeCrAl heating wire 2 Ω, current 7 A; **c** first-order reaction plots for PE degradation during the wet reforming and decomposition; **d** Arrhenius relationships between rate constants and temperature; **e** the contribution of H_2O to H_2 yield in water decomposition and wet reforming of PE; and **f** FTIR spectra of gas products at different reaction intervals in wet reforming of PE, PE 14 mg, H_2O 30 μL, FeCrAl heating wire 2 Ω, current 7 A.

0.2546 min^{-1} according to the slope value of ln(1/a) - t plot, which is larger than that in PE dehydrogenation (0.1043 min^{-1}). Furthermore, systematic kinetic investigations were conducted across a range of reaction temperatures by precisely regulating the current flow through the heating wire. The results demonstrate that the rate constants for PE degradation in both wet reforming and dehydrogenation of PE exhibit a pronounced temperature dependence, which can be well described by the Arrhenius equation (Fig. 3d). The lower apparent activation

energy (14.08 kJ•mol^{-1}) of PE degradation in wet reforming of PE than the one (25.17 kJ•mol^{-1}) in PE degradation indicates the different degradation pathway of PE in the two processes. According to the data for plotting the Arrhenius equation of wet reforming of PE, a relationship between syngas yield (Y: %), electrified power (P: W), temperature (T: K), and reaction time (t: min) can be derived. Based on this equation (Eq. 1), the syngas yield can be determined under the conditions of sufficient reactant availability and kinetic-controlled

reaction regime.

$$Y = 0.0349P + 0.8706T + 30.34t - 1.396 \times 10^3 PT - 766.144 \quad (1)$$

The contribution of water to H_2 yield can be calculated by subtracting the H_2 yields produced by PE decomposition from those produced during the wet reforming of PE (Fig. 3e), thereby quantifying the amount of H_2 derived from water. We also investigated the water decomposition over the electrified heating wire at the same time points. It was found that the H_2 yields of water decomposition in the initial phase (1 min and 3 min) were higher than those obtained by water decomposition in wet reforming of PE, but significantly lower than those in the latter stages of the reactions (Fig. 3e). Furthermore, the weight of the heating wire increased slightly after the water decomposition (Supplementary Table 8). Therefore, it can be concluded that the electrified heating wire can promote H_2 production from water by taking away oxygen from water at the initial stage of the reaction. Surface oxidation of the heating wire reduces its capacity to extract oxygen from water over time, leading to lower activity in producing H_2 through water decomposition. However, in conjunction with PE dehydrogenation, the oxygen coated on the surface of the heating wire can be removed in the form of CO by the carbon species generated during PE dehydrogenation, resulting in a significant contribution to H_2 production from water in the final half-stage of wet reforming of PE.

The FTIR spectra of gaseous products at different reaction intervals further demonstrate the mutual promotion between PE and water decomposition (Fig. 3f and Supplementary Fig. 7). Under the normal reaction conditions, the characteristic vibrations of CO ($2100-2200 \, cm^{-1}$) and gaseous hydrocarbons ($2850-3200 \, cm^{-1}$) were detected as early as 10 s after electrification. After 1 min, the intensity of the two types of signals was obviously strong, and then increased with increasing reaction time (Fig. 3f). In contrast, when no water was present in the reaction system, the signal intensity of gaseous hydrocarbons at $2850-3200 \, cm^{-1}$ was weak even after 1 min of electrification (Supplementary Fig. 7). With the extension of electrification time, the characteristic vibration of gaseous hydrocarbons gradually became stronger, and the weak vibration of CO did not increase obviously because the finite oxygen in the system can only be provided by the heating wire. The experiments also demonstrate that PE first decomposed into gaseous hydrocarbons under the thermal irradiation of the electrified heating wire, and the produced hydrocarbons subsequently reformed with H_2O to produce syngas. The presence of H_2O can promote PE decomposition. Correspondingly, attenuated total reflection Fourier-transform infrared (ATR-FTIR) analysis of residues at different reaction times indicates that the duration of PE decomposition in the absence of water was about 3 min, longer than the time (about 1 min) in the presence of water (Supplementary Figs. 8 and 9). However, the FTIR analysis cannot provide evidence for H_2O decomposition promoted by PE decomposition because the hydrogen molecule lacks IR-active characteristic vibrations.

The kinetics of wet reforming and dehydrogenation processes of PS, as well as PET, were also systematically investigated (Fig. 4). In the wet reforming of PS (Fig. 4a), the residual solid content decreased to 61% after just 1 min of heating wire activation (Supplementary Fig. 10), with concurrent production of 28% CO, 14% H_2, 19% C_{2+} and trace amount of CH_4 and CO_2. Notably, the C_{2+} hydrocarbon contains fused-ring compounds according to GC-MS analysis (Supplementary Fig. 11), and the residual solid was black coke. At the reaction time of 3 min, the residual solid was only 32%, and the yields of H_2 and CO increased to 25% and 49%. The yield of C_{2+} products decreased slightly, and the contents of CH_4 and CO_2 showed no obvious change. By 9 min, the consumption rate of residual solids decreased obviously, and the yield of C_{2+} products decreased, along with the increase of H_2 and CO yields. After that, the decrease rate of residual coke yield and the increase rate

of H_2 and CO yields both obviously decreased, while the CO_2 yield increased slightly. The dehydrogenation kinetics of PS (Fig. 4b) demonstrated rapid H_2 generation during the initial 3 min, approaching the theoretical yield by 3 min. The residual solid mass showed a decrease in the initial stage and a slight increase at the final stage. The C_{2+} products can also be detected at the reaction of 1 min. The morphology of coke derived from wet reforming of PS is similar to that obtained from PS dehydrogenation (Supplementary Fig. 12), both exhibiting a nanosphere structure. These results demonstrate that both wet reforming and dehydrogenation of PS have a fast dehydrogenation rate. The existence of phenyl groups in PS enhances the production of fused-ring compounds and accelerates coke formation under Joule heating conditions. PET wet reforming kinetics (Fig. 4c) similarly exhibited a fast initial reaction rate. At the reaction time of 1 min, the residual solid was left 66%, and the yields of CO and H_2 reached to 36% and 10%. At the reaction time of 3 min, only 28% solid was left, and the yield of CO increased to 60%, while the H_2 yield was only 15%. After that, the reforming rate slowed down as both the consumption rate of residual solid and the increase rate of syngas yield declined, which mainly involves the wet reforming process. The C_{2+} products can be detected at the reaction time of 1 min, mainly composed of fused-ring compounds and terephthalic acid derivatives according to GC-MS analysis (Supplementary Fig. 13). The residual coke cannot be reformed completely even the reaction time was 18 min (Supplementary Fig. 14). If there was no water in the system, the reaction should be PET decomposition (Fig. 4d). At the reaction time of 1 min, the CO yield has reached to 13% and H_2 yield was 48%, demonstrating the CO was generated from PET decomposition directly. At 3 min, the H_2 and CO yields increased to 62% and 25%, respectively. After that, the mass of residual solid decreased slowly, and the syngas yield increased gradually. Finally, about 48% solid was left, which has similar morphology to that obtained from the wet reforming of PET (Supplementary Fig. 15). The first-order kinetic plots derived from PS and PET wet reforming and dehydrogenation processes (Fig. 4e, f) consistently demonstrate higher rate constants for wet reforming compared to dehydrogenation or decomposition pathways.

To further clarify the wet reforming mechanism, isotope-labeling experiments were carried out using deuterium water (D_2O) and PE as reactants. The hydrogen in the gas products at different electrification times was sampled and analyzed using a mass spectrometer (MS, Supplementary Fig. 16). The signals $m/z = 2$, 3, and 4 corresponded to H_2, HD, and D_2, respectively, demonstrating the involvement of PE and D_2O in the hydrogen production process. As shown in Fig. 5a, after 1 min of electrification, only the $m/z = 4$ signal was detected, indicating that water decomposition occurred first and PE has no contribution to hydrogen production in the initial stage of wet reforming of PE. As the electrification time increased, for example, 3 min after electrification, the signals $m/z = 2$ and $m/z = 3$ appeared and were stronger than $m/z = 4$, indicating that PE dehydrogenation occurred and mainly contributed to hydrogen production. The presence of a strong signal $m/z = 3$ indicated an effective combination of H atom from PE and D from D_2O during the reforming process, which may be due to the proton hopping mechanism on the surface of the electrified heating wire. That is, some hydroxyls (-OD) and protons (D) generate on the electrified heating wire during water decomposition in the initial stage collide with gaseous hydrocarbons derived from PE decomposition and capture H from these hydrocarbons to generate HD. In contrast, when H_2O was used instead of D_2O, the signal $m/z = 2$ was detected at a reaction time of 1 min and signals for $m/z = 3$ and 4 were absent throughout the entire process (Supplementary Fig. 16). To prove the generation of hydroxyls or protons on the surface of heating wire, a temperature-programmed desorption (TPD) experiment was designed and the desorbed hydrogen can be detected by an on-line MS (Fig. 5b and Supplementary Fig. 17). Before TPD analysis, the heating wire was first electrified in the presence of $30 \, \mu L \, H_2O$ or D_2O. The signal
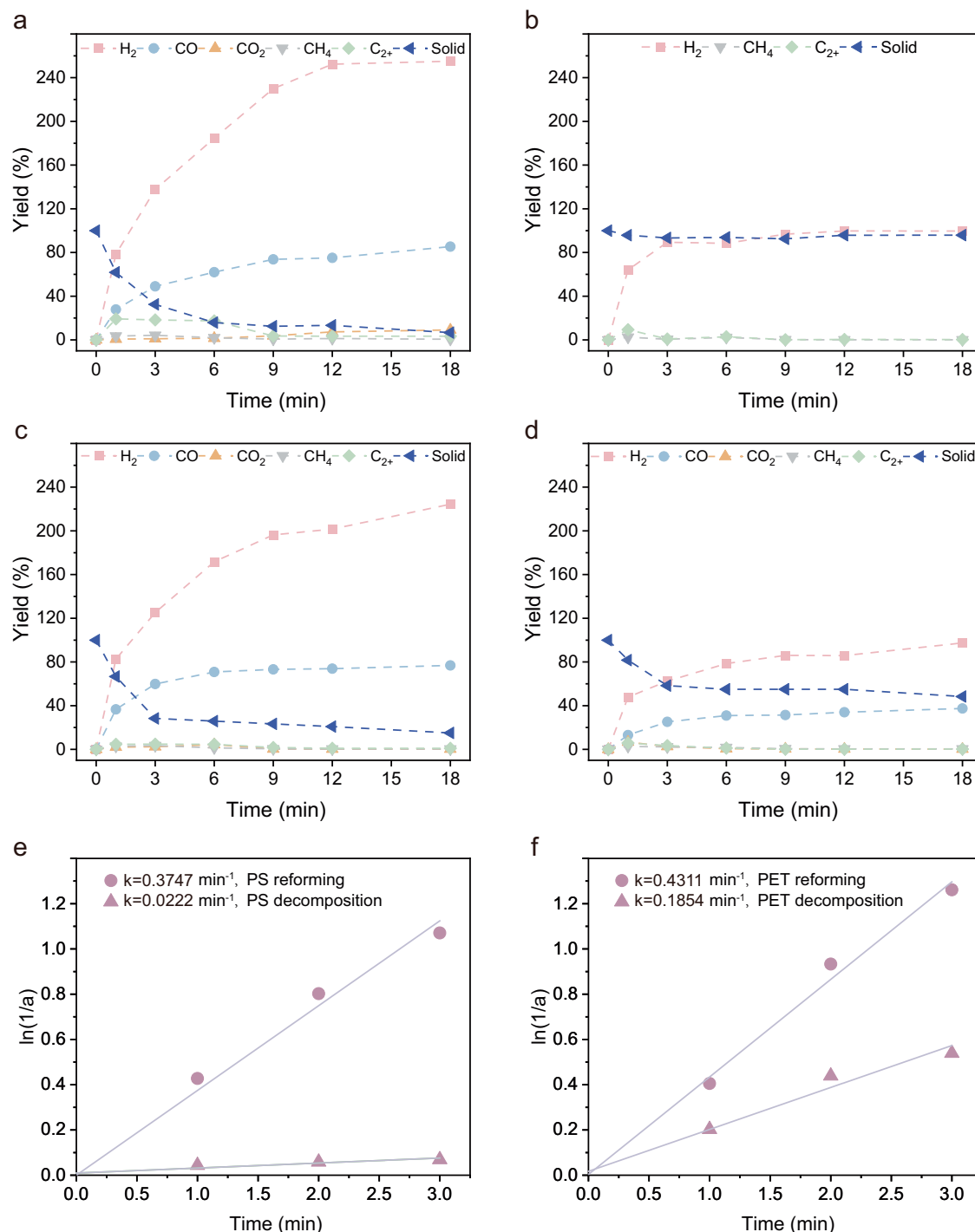
Fig. 4 | Kinetic studies of PS and PET wet reforming and dehydrogenation processes. a Kinetic analysis of wet reforming of PS, Reaction conditions: PS 13 mg, H_2O 40 μL, FeCrAl heating wire 2 Ω, current 7 A; **b** kinetic analysis of decomposition of PS Reaction conditions: PS 13 mg, FeCrAl heating wire 2 Ω, current 7 A; **c** kinetic analysis of wet reforming of PET, Reaction conditions: PET 19.2 mg, H_2O 50 μL, FeCrAl heating wire 2 Ω, current 7 A; **d** kinetic analysis of PET decomposition, reaction conditions: PET 19.2 mg, FeCrAl heating wire 2 Ω, current 7 A; **e** first-order reaction plots for PS degradation in wet reforming process and decomposition process; and **f** first-order reaction plots for PET degradation in wet reforming process and decomposition process.

for $m/z = 2$ was detected when the H_2O-treated heating wire was loaded into the TPD furnace at $T = 337$ °C, and no signals for $m/z = 3$ and $m/z = 4$ were observed during the whole process (Supplementary Fig. 18). For the D_2O-treated heating wire, the signal for $m/z = 4$ was observed at $T = 247$ °C except for the weak signals for $m/z = 2$ and $m/z = 3$, which may result from the trace of H_2O in D_2O (Fig. 5b). The TPD-MS experiments suggest the generation of hydrogen-containing species such as hydroxyls or protons on the surface of heating wire

during the experiments, further demonstrating the rationality of the proton hopping mechanism of the reforming process. Scanning electron microscopy-energy dispersive X-Ray spectroscopy (SEM-EDS) analyses further demonstrated that the oxygen content on the surface of the heating wire increased obviously after reaction (Supplementary Figs. 19 and 20). Based on the isotope-labeling experiments, a reasonable reaction mechanism can be proposed[36]. In the initial stage, the high temperature caused by the heating wire promoted the pyrolysis
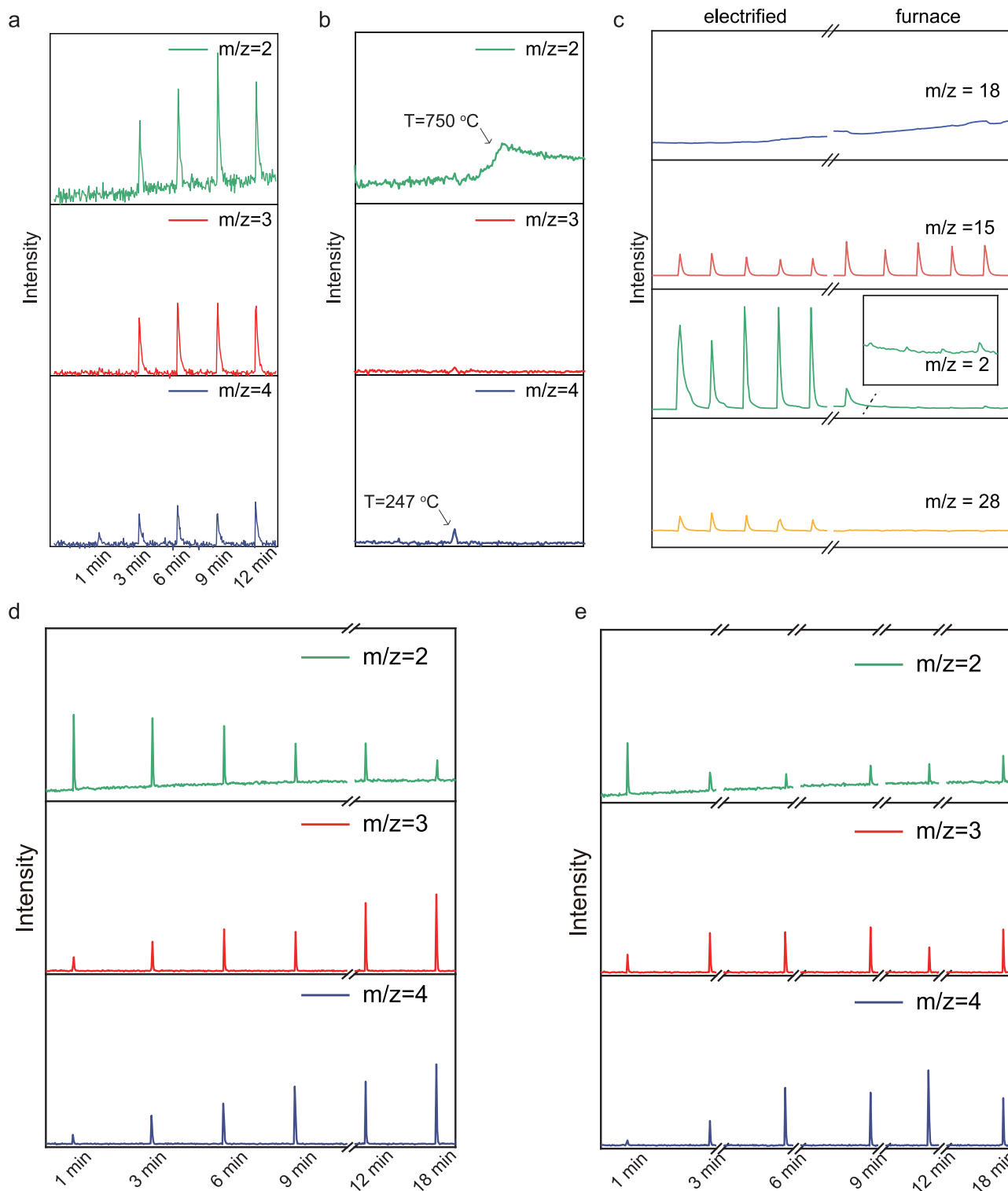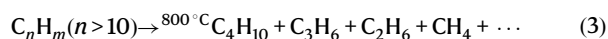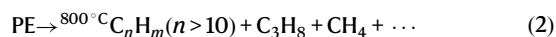
Fig. 5 | Mechanistic studies of wet reforming of plastics. a MS signals of wet reforming PE with 30 μL D_2O at different reaction times; **b** MS signals of TPD research for FeCrAl heating wire pre-treated by 30 μL D_2O; **c** MS signals of pulsed wet reforming of methane over electrified heating wire and non-electrified heating wire. Reaction conditions: carrier gas (Ar) 20 mL/min, pulsed gas: methane 10 mL/ min and argon gas flow through H_2O 10 mL/min, FeCrAl heating wire 2 Ω, current 7 A; **d** MS signals of wet reforming of PS with 40 μL of D_2O at different reaction times; and **e** MS signals of wet reforming PET with 50 μL D_2O at different reaction times.

of PE into low molecular weight hydrocarbons (Eqs. 2 and 3), such as methane, ethane, propane, and even hexane. These hydrocarbons have been detected by GC. At the same time, water was gasified into steam and decomposed into active hydrogen radicals, oxygen radicals, hydroxyls, or hydrogen on the electrified heating wire (Eqs. 6−9). Then, the gaseous hydrocarbons can be reformed into H_2 and CO via the proton hopping mechanism on the electrified heating wire (Eqs. 10−15).

a Decomposition steps

$$PE \xrightarrow{800\,^\circ C} C_nH_m(n>10) + C_3H_8 + CH_4 + \cdots \qquad (2)$$

$$C_nH_m(n>10) \xrightarrow{800\,^\circ C} C_4H_{10} + C_3H_6 + C_2H_6 + CH_4 + \cdots \qquad (3)$$

$$PS \xrightarrow{800\,^\circ C} H_2 + C + \text{fused ring} + CH_4 + \cdots \qquad (4)$$

$$PET \xrightarrow{800\,^\circ C} H_2 + C + CO + \text{fused ring} + CH_4 + \cdots \qquad (5)$$

b Hopping steps

$$D_2O + * \leftrightarrow D_2O* \qquad (6)$$

$$D_2O* + * \rightarrow OD* + D* \qquad (7)$$

$$OD* + * \rightarrow O* + D* \qquad (8)$$

$$D* + D* \rightarrow D_2 + 2* \qquad (9)$$

c Reforming steps

$$CH_4 + D* \rightarrow CH_3* + HD \qquad (10)$$

$$CH_3* + * \leftrightarrow CH_2* + H* \qquad (11)$$

$$CH* \rightarrow C + H* \qquad (12)$$

$$H* + H* \rightarrow H_2 + 2* \qquad (13)$$

$$H* + D* \rightarrow HD + 2* \qquad (14)$$

$$C + O* \rightarrow CO + * \qquad (15)$$

To further prove the importance of the proton hopping mechanism in the electrical field, a pulse experiment of wet reforming of methane monitored by in-situ MS was carried out (Fig. 5c and Supplementary Fig. 21). On the electrified heating wire, methane can be reformed with H_2O to H_2 ($m/z = 2$) and CO ($m/z = 28$). However, over the unelectrified heating wire heated by a furnace, the signal $m/z = 2$ representing hydrogen can only be detected obviously after the first pulse, and the signal of CO ($m/z = 28$) did not appear. Thereafter, the hydrogen signals from the non-electrified heating wire diminished significantly, and no CO was detected. These results show that the hydrogen was produced by water decomposition on the non-electrified heating wire at high temperature. However, the oxygen-containing groups on the non-electrified heating wire cannot react with methane and produce syngas even at high temperatures. The pulse methane wet reforming experiment demonstrate the importance of electrification, which maintains the high catalytic activity of the heating wire and promotes catalytic recycling.

The isotope-labeling experiments were also conducted to investigate the wet reforming of PS and PET in the presence of D_2O (Fig. 5d, e). At the initial stage of electrification, the mass signals for $m/z = 2$, 3, and 4 were all detected, and the intensity of $m/z = 2$ was strong, indicating that the PS dehydrogenation, PET dehydrogenation, and water decomposition occurred. The hydrogen radicals from PS or PET

combined with deuterium radicals to generate HD instantly. After that, the intensity of $m/z = 2$ decreased while the intensity of $m/z = 3$ and 4 increased. It demonstrates that the dehydrogenation occurred firstly due to the presence of phenyl groups in PS and PET, and the generated coke and fused-ring compounds reformed with D_2O subsequently to produce H_2, HD, D_2, and CO. These results are consistent with the kinetic studies.

Energy recovery efficiency and life cycle assessment

This Joule heating-promoted wet reforming system utilizes waste plastic and water as reactants to produce syngas, with electrical energy as the primary energy input. To evaluate the energy recovery efficiency (ERE) of the system, an electric meter was used to measure the electricity consumption during the reaction, and the energy embodied in the products can also be calculated (Supplementary Tables 9 and 10). The ERE of the reforming system using the scaled-up stainless-steel reactor was determined to be 4.11% (Fig. 6a), which is notably higher than that of other reported systems, such as the conventional wet reforming system (1.91%) and Joule heating-promoted dry reforming of PE (0.6%)[26]. In addition, the GHG emission and primary fossil energy (PFE) depletion are primarily attributed to the power generation process. According to the life cycle assessment (LCA) performed using GREET 2024 (Supplementary Tables 11 and 12), when powered by the current world average electricity mix, the reforming system generates 349.36 kg CO_2 eq of GHG emissions and consumes 7368 MJ of PFE per 1 kg of syngas produced under optimal conditions (Fig. 6a). To improve the sustainability of system, a demonstration reforming setup powered by photovoltaic (PV) electricity under natural sunlight was established (Fig. 6b, Supplementary Figs. 22 and 23). With this renewable energy source, GHG emissions and PFE depletion were reduced by 94.48% and 93.66%, respectively, while the ERE increased dramatically to 125.1%. Consequently, the PV-powered Joule heating-promoted wet reforming system exhibits significantly lower GHG emission and PFE depletion, along with higher energy recovery efficiency, compared to both the conventional wet reforming system and the Joule heating-promoted dry reforming system (Supplementary Tables 13 and 14). Therefore, this solar-energy-driven wet reforming system for plastics can be considered a green and efficient strategy to solve the environmental problem and store solar energy in the form of chemical energy in syngas.

Discussion

Wet reforming of plastics was achieved over an electrified commercial heating wire through Joule heating. Real waste plastic containing residual water was directly converted into H_2 and CO. A stainless-steel T-type reactor can tolerate high pressure and has a feed inlet, allowing the batch reaction to be continuous, and converting 2.5 g PE plastic and 5.5 g water to 3.1 g syngas. Compared to conventional thermal catalysis and plasma catalysis, the proposed Joule heating strategy exhibits three fundamental advantages:

1) Enhanced energy utilization efficiency. The Joule heating mechanism directly converts electrical energy into thermal energy through resistive heating, enabling efficient heat transfer to the reactants via conduction and convection within the reactor chamber. In contrast, conventional heating methods inevitably involve heat transfer from external sources through the reactor walls, resulting in significant thermal losses. Plasma systems require energy-intensive voltage conversion (1 V → 10 kV) and specialized discharge circuits, with significant energy consumption in the conversion and discharge processes.

2) Faster heating rate. The Joule heating process can rapidly heat the reactants to 800 °C within just 30 s, whereas conventional furnaces typically require at least 30 min to reach the same temperature. This rapid heating promotes efficient cracking of C−C and C−H bonds in plastics while minimizing undesirable side
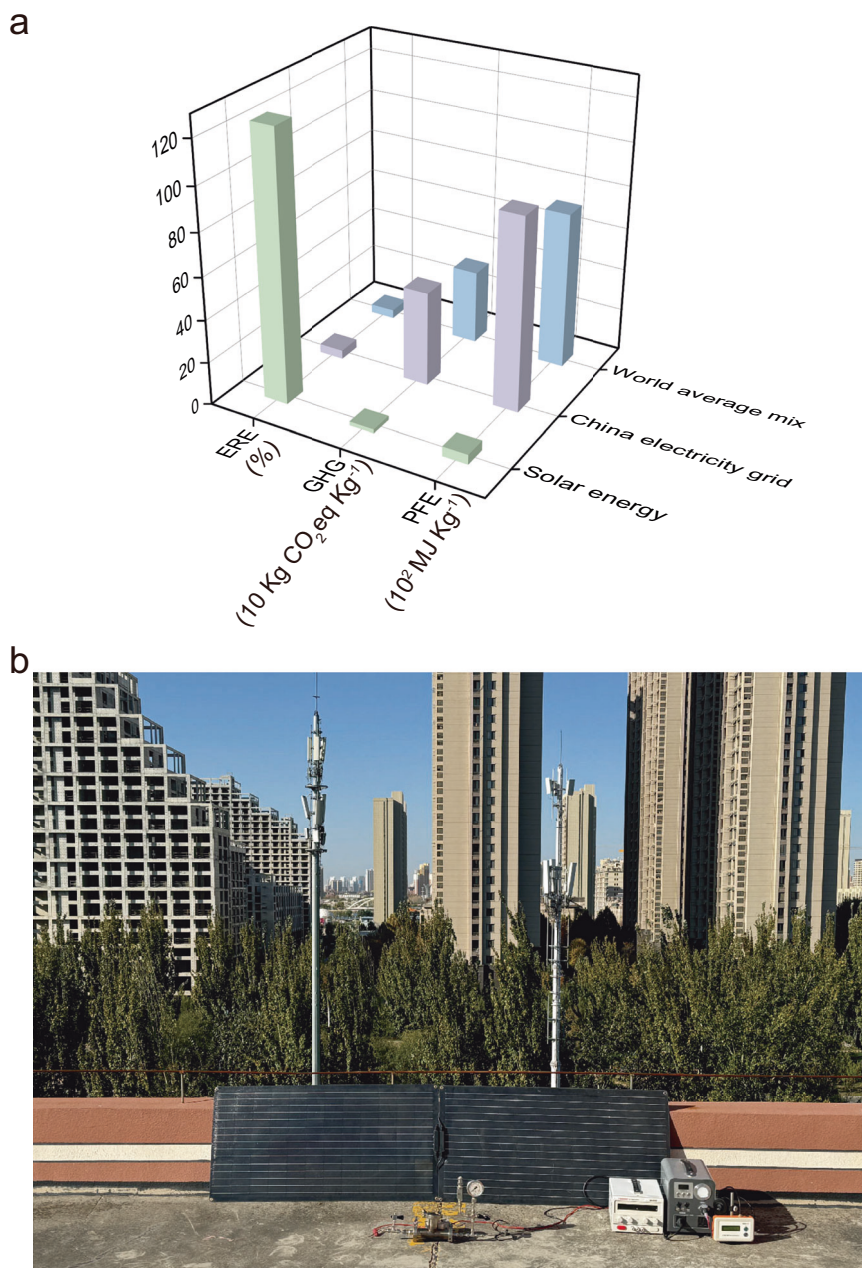
Fig. 6 | Life cycle analyses and a large-scale Joule heating system powered by solar. a GHG emissions, PFE consumption, and energy recovery efficiency of the Joule heating reforming system for producing 1 kg syngas; **b** wet reforming of waste plastics powered by a PV power system, reaction conditions: PE bag 0.25 g, H_2O 550 μL, FeCrAl heating wire 4 Ω, current 7 A, 25 min.

reactions. Therefore, the CO yield in the Joule heating-promoted wet reforming of plastics is higher than 95%, and the H_2 yield is almost twice that of CO, which is higher than the conventional reforming processes.

3) Lower production cost. The Joule heating system utilizes a simple FeCrAl heating wire as both heating element and catalytic component, which is commercially available at low cost. The system requires only a standard direct current (DC) power supply without any specialized equipment. In comparison, conventional two-stage pyrolysis-reforming processes necessitate expensive reforming catalysts and multiple heating furnaces, while plasma catalysis systems require costly high-voltage generators and specialized electrodes capable of withstanding plasma conditions.

Kinetic studies and isotope-labeling MS experiments revealed that hydrogen production in the initial stage of the wet reforming of PE primarily resulted from the water decomposition, rather than from plastic dehydrogenation. The active oxygen or hydroxyl species present on the surface of the heating wire reacted with gaseous hydrocarbons derived from the PE decomposition to generate hydrogen and CO. However, for plastics containing phenyl groups, such as PS and PET, dehydrogenation occurred preferentially, leading to the formation of fused-ring compounds or coke. Subsequently, the coke or fused-ring species reacted with water to produce syngas. Furthermore, the wet reforming of plastics can be achieved under solar irradiation with a photovoltaic power system. Therefore, the Joule heating-promoted wet reforming system for converting plastic and water to syngas can be seen as an efficient measure to store solar energy and

develop the carbon/hydrogen resources contained in waste plastic and water with high energy recovery efficiency.

Compared to the Joule heating-promoted dry reforming of plastics[26], this work makes great advances and innovations as follows (Supplementary Table 15):

1) The T-type reactor in this work features a dedicated feeding inlet, which makes it much easier to introduce reactants into the reactor and to run a batch reaction continuously. The large-scale stainless-steel T-type reactor, equipped with a pressure gauge and relief valve, can withstand elevated pressure levels and ensures operational safety.

2) The isotope-labeling MS experiments in this research provide valuable mechanistic insight. A similar experiment should be designed to investigate the Joule heating-promoted dry reforming of plastics.

3) The wet reforming of plastic is different from the dry reforming of plastic, possessing higher atom utilization efficiency and producing hydrogen-rich syngas. The presence of steam in the Joule heating system can produce more hydroxyls on the surface of electrified heating wire, making the proton-hopping mechanism easier than in the dry reforming process. Consequently, the wet reforming of plastics demonstrates significantly higher energy recovery efficiency compared to the dry reforming process. Notably, real-world plastic waste, even when contaminated with food residues, paints, oils, and greases, can be effectively reformed into syngas in the wet reforming system, demonstrating significant potential for practical applications in plastic waste upcycling.

Inspired by the remarkable performance of Joule heating-promoted wet and dry reforming of plastics, a combined reforming process utilizing plastic waste, carbon dioxide, and water as reactants emerges as a highly promising approach. Notably, the H_2/CO ratio in the produced syngas can be precisely tuned to meet specific industrial requirements by simply adjusting the water content in the feedstock.

Methods

Materials
PE (powder with size 1000 mesh) and PP ($M_W = 42.08$) were obtained from Shanghai Macklin Biochemical Technology Co., Ltd. PET (300 mesh) was obtained from Shanghai Branch, Du Pont China Holding Co., Ltd. Isotopic D_2O was supplied by chemical supplier (Shanghai Titan Scientific Co.,Ltd). All chemicals were used without any further purification and dry.

Wet reforming of PE
The wet reforming of plastic was carried out in a custom-made T-type quartz tube reactor, which has an inner diameter of 19 mm, an outer diameter of 25 mm, a main pipe length of 100 mm, and a side pipe length of 60 mm. The three ends of the T-type quartz tube were fitted with three sets of stainless-steel flanges. Two of these flanges, located on the main pipe, were equipped with ball valves, while the third was sealed with a blind plate. Plastic could be directly introduced into the reactor through this inlet. A porcelain boat with dimensions (44 mm × 11 mm × 7 mm) was utilized to both load the plastic and to support the heating wire. Prior to the reaction, 14 mg of polyethylene (PE) and 30 μL of water (H_2O) were placed into the boat, and a spring-like heating wire with a resistance value of 2 Ω was installed above it. Subsequently, two copper wires, which passed through the flanges, were connected to the ends of the heating wire. The porcelain boat, equipped with the heating wire, was positioned at the midpoint of the quartz tube and was sealed into the tube using flanges. The reactor was connected to an argon gas pipeline and purged with argon gas at a flow rate of 20 mL/min for 20 min. Once the two valves were closed, the argon gas remaining within the reactor at atmospheric pressure was used as an internal standard to quantify the other gaseous products formed after the reaction. The terminals of a direct-current power supply (MAISHENG, MP3030D) were connected to the two copper wires, and the heating wire was energized by adjusting current or voltage to reach a red-hot state, providing the thermal energy required for the wet reforming reaction. After reaction, the gas products were sampled by a syringe through a valve and analyzed with a gas chromatography (Agilent 7820A) equipped with a thermal conductivity detector (TCD) and flame ionization detector (FID). At the initial stage of reforming reaction, the structure of compounds generated from plastics (PE, PS, and PET) was determined by gas chromatography mass spectrometry (GC-MS, Agilent 8860-5977B).

The large-scale experiments were conducted in a T-type stainless-steel reactor, which was equipped with two ball valves and electrodes. A side tube inlet was strategically designed to introduce reactants after the completion of each batch of reactions. The reactor was coated with thick thermal insulation to minimize energy loss during the reaction. To prevent an electrical short circuit, a quartz boat was specifically designed to support the heating wire and to hold the waste plastics during the reaction. Argon gas was introduced into the reactor and served as an internal standard for quantifying the gaseous products.

Fourier transform infrared spectroscopy (FTIR) analysis
The FTIR analysis of gas products was performed in a gas chamber that featured two side windows made of zinc selenide and a top window fabricated from quartz. The zinc selenide windows facilitate the transmission of the laser through the chamber, enabling the gas to be analyzed using FTIR spectroscopy. The chamber was purged with argon gas to remove air, and a background spectrum was recorded prior to analysis. The gas product at different reaction times was sampled reactor and injected into the gas chamber for analysis.

In-situ mass spectrography (MS) analysis
The in-situ MS experiments were carried out with methane as a model hydrocarbon and argon as a carrier gas on a mass spectrometer (Hiden, HPR-40). A length of heating wire connected with a wire was fixed in a quartz tube (inner diameter: 6 mm) and can be powered by a direct-current power (MAISHENG, MP3030D). At the end of the quartz tube, there was a triple bypass connected to the MS and tailpipe. The products can then be monitored by the online MS. A six-way valve having a quantitative ring was used to pulse methane and/or wet into the quartz tube. In the in-situ experiments, the signals of argon ($m/z = 40$), H_2 ($m/z = 2$), H_2O ($m/z = 18$), CO ($m/z = 28$), and CH_4 ($m/z = 15$) were set to be monitored by MS.

Isotope-labeling experiments
The PE/PS/PET reforming experiments with D_2O or the mixture of H_2O and D_2O were carried out in a quartz reactor. The gas products at different reaction intervals were sampled and analyzed by MS. After the baselines of MS signals H_2 ($m/z = 2$), HD ($m/z = 3$), and D_2 ($m/z = 4$) were stable, the gas product at different reaction intervals was injected in to MS through a six-way valve having a quantitative ring.

Carbon balance and mass balance calculations
With argon gas as an internal standard, the yield of gas products (such as H_2, CO, CO_2, CH_4 and C_{2+}) can be quantified by gas chromatography (Agilent 7820A) equipped with a FID and a thermal conductivity detector (TCD). Then the residual solid (m_{solid}) can be quantified by weighing the reactor before and after reaction. Therefore, the carbon balance can be calculated.

$$\text{Carbon balance} = \frac{n_{CO} + n_{CO_2} + 2n_{C_2H_x} + 3n_{C_3H_x} + \frac{m_{solid}}{12}}{\frac{m_{PE}}{14}} \times 100\% \quad (16)$$

Here, n_i represent the molar number of gas products. The residual solid in reactor after reaction was seen as carbon. Thus, the molar number of carbon in residual solid was calculated by $m_{solid}/12$.

The mass balance calculation was based on the observable products (H_2, CO, CO_2, CH_4, C_{2+} and solid), and the formula is shown below:

$$\text{Mass balance} = \frac{2n_{H_2} + 28n_{CO} + 44n_{CO_2} + 16n_{CH_4} + Mn_{C_{2+}} + m_{solid}}{m_{PE} + m_{H_2O}(\text{actual})} \times 100\% \tag{17}$$

where M is the relative molecular mass of different products. Moreover, the value of m_{H_2O} (actual) is determined by the mass of CO_2 and CO, since H_2O is the only oxygen source in the reforming system. At the same time, the H_2 of syngas came from PE dehydrogenation and H_2O decomposition. Besides, the yields of H_2 and X (CO, CO_2, CH_4, C_{2+} and solid) were calculated from:

$$\text{Yield}_{H_2} = \frac{n_{H_2}(\text{quantified on GC})}{n_{H_2}(\text{in plastic})} \times 100\% \tag{18}$$

$$\text{Yield}_X = \frac{n_X(\text{quantified on GC or balance})}{n_X(\text{in plastic})} \times 100\% \tag{19}$$

Life cycle assessment

The analysis was performed in GREET 2024 software. The life cycle inventory (LCI) for the reforming system is shown in Supplementary Table 11, which involves the product item, category, and quantity. We assume a certain mass for the plastic waste, adapt to a certain amount of H_2O and electricity, and run the LCA calculation. The study applied a functional unit of 1 kg of syngas. This process is equipped with various chemicals (H_2O), as well as electricity. The life cycle inventory list of the inputs and outputs achieved from GREET 2024 is presented in Supplementary Table 12.

Data availability

The data that support the Figures within this paper and other findings of this study are available from the corresponding author upon request. Source data are provided as a Source Data file. Source data are provided with this paper.

References

1. Sansaniwal, S. K., Pal, K., Rosen, M. A. & Tyagi, S. K. Recent advances in the development of biomass gasification technology: a comprehensive review. *Renew. Sust. Energ. Rev.* **72**, 363–384 (2017).
2. Abdulrasheed, A. et al. A review on catalyst development for dry reforming of methane to syngas: recent advances. *Renew. Sust. Energ. Rev.* **108**, 175–193 (2019).
3. Gopinath, K. P., Nagarajan, V. M., Krishnan, A. & Malolan, R. A critical review on the influence of energy, environmental and economic factors on various processes used to handle and recycle plastic wastes: development of a comprehensive index. *J. Clean Prod.* https://doi.org/10.1016/j.jclepro.2020.123031 (2020).
4. Wang, M. et al. A triple increase in global river basins with water scarcity due to future pollution. *Nat. Commun.* https://doi.org/10.1038/s41467-024-44947-3 (2024).
5. Mitch, W. A., Richardson, S. D., Zhang, X. & Gonsior, M. High-molecular-weight by-products of chlorine disinfection. *Nat. Water* **1**, 336–347 (2023).
6. Lee, K., Jing, Y., Wang, Y. & Yan, N. A unified view on catalytic conversion of biomass and waste plastics. *Nat. Rev. Chem.* **6**, 635–652 (2022).
7. Alabi, O., Ologbonjaye, K., Awosolu, O. & Alalade, O. Public and environmental health effects of plastic wastes disposal: a review. *J. Toxicol. Risk Assess.* https://doi.org/10.23937/2572-4061.1510021 (2019).
8. Geyer, R., Jambeck, J. R. & Law, K. L. Production, use, and fate of all plastics ever made. *Sci. Adv.* https://doi.org/10.1126/sciadv.1700782 (2017).
9. Ellis, L. D. et al. Chemical and biological catalysis for plastics recycling and upcycling. *Nat. Catal.* **4**, 539–556 (2021).
10. Lovás, P., Hudec, P., Jambor, B., Hájeková, E. & Horňáček, M. Catalytic cracking of heavy fractions from the pyrolysis of waste HDPE and PP. *Fuel* **203**, 244–252 (2017).
11. Nixon, K. D. et al. Analyses of circular solutions for advanced plastics waste recycling. *Nat. Chem. Eng.* **1**, 615–626 (2024).
12. Williams, E. A. & Williams, P. T. Analysis of products derived from the fast pyrolysis of plastic waste. *J. Anal. Appl. Pyrolysis* **40-41**, 347–363 (1997).
13. Feng, S., Nguyen, P. T. T., Ma, X. & Yan, N. Photorefinery of biomass and plastics to renewable chemicals using heterogeneous catalysts. *Angew. Chem. Int. Ed.* https://doi.org/10.1002/anie.202408504 (2024).
14. Dong, Z. et al. Understanding the structure–activity relationships in catalytic conversion of polyolefin plastics by zeolite-based catalysts: a critical review. *ACS Catal.* **12**, 14882–14901 (2022).
15. Yuan, S. et al. Highly active sunlight-driven CO_2 methanation catalyst: design of the interfacial structure. *Fuel* https://doi.org/10.1016/j.fuel.2022.126855 (2023).
16. Yuan, S. et al. CO_2 methanation boosted by support-size-dependent strong metal-support interaction and B–O–Ti component. *Green. Energy Environ.* **9**, 321–332 (2024).
17. Wang, M. et al. Complete hydrogenolysis of mixed plastic wastes. *Nat. Chem. Eng.* **1**, 376–384 (2024).
18. Liang, X., Wang, M. & Ma, D. One-pot conversion of polyester and carbonate into formate without external H_2. *J. Am. Chem. Soc.* **146**, 2711–2717 (2024).
19. Zhang, M.-Q. et al. Catalytic strategies for upvaluing plastic wastes. *Chem* **8**, 2912–2923 (2022).
20. Sun, J. et al. Catalytic upcycling of polyolefins. *Chem. Rev.* **124**, 9457–9579 (2024).
21. Qin, B. & Zhang, X. On depolymerization. *CCS Chem.* **6**, 297–312 (2024).
22. Wismann, S. T. et al. Electrified methane reforming: a compact approach to greener industrial hydrogen production. *Science* **364**, 756–759 (2019).
23. Yao, D., Yang, H., Chen, H. & Williams, P. T. Investigation of nickel-impregnated zeolite catalysts for hydrogen/syngas production from the catalytic reforming of waste polyethylene. *Appl. Catal. B* **227**, 477–487 (2018).
24. Williams, P. T. Hydrogen and carbon nanotubes from pyrolysis-catalysis of waste plastics: a review. *Waste Biomass. Valoriz.* **12**, 1–28 (2020).
25. Song, C., Wang, Z., Yin, Z., Xiao, D. & Ma, D. Principles and applications of photothermal catalysis. *Chem. Catal.* **2**, 52–83 (2022).
26. Ma, Q. et al. Grave-to-cradle dry reforming of plastics via Joule heating. *Nat. Commun.* https://doi.org/10.1038/s41467-024-52515-y (2024).
27. Acomb, J. C., Wu, C. & Williams, P. T. Control of steam input to the pyrolysis-gasification of waste plastics for improved production of hydrogen or carbon nanotubes. *Appl. Catal. B* **147**, 571–584 (2014).
28. Zhang, X. et al. CO2-mediated catalytic upcycling of plastic waste for H2-rich syngas and carbon nanomaterials. *J. Hazard. Mater.* https://doi.org/10.1016/j.jhazmat.2023.132500 (2023).
29. Dong, Q., Hu, S. & Hu, L. Electrothermal synthesis of commodity chemicals. *Nat. Chem. Eng.* https://doi.org/10.1038/s44286-024-00134-1 (2024).

30. Aminu, I., Nahil, M. A. & Williams, P. T. Hydrogen production by pyrolysis–nonthermal plasma/catalytic reforming of waste plastic over different catalyst support materials. *Energy Fuels* **36**, 3788–3801 (2022).

31. Zhang, Y., Huang, J. & Williams, P. T. Fe–Ni–MCM-41 catalysts for hydrogen-rich syngas production from waste plastics by pyrolysis—catalytic steam reforming. *Energy Fuels* **31**, 8497–8504 (2017).

32. Li, Y., Nahil, M. A. & Williams, P. T. Hydrogen/syngas production from different types of waste plastics using a sacrificial tire char catalyst via pyrolysis–catalytic steam reforming. *Energy Fuels* **37**, 6661–6673 (2023).

33. Al-Fatesh, A. S. et al. From plastic waste pyrolysis to Fuel: Impact of process parameters and material selection on hydrogen production. *Fuel* https://doi.org/10.1016/j.fuel.2023.128107 (2023).

34. Aminu, I., Nahil, M. A., & Williams, P. T. Pyrolysis-plasma/catalytic reforming of post-consumer waste plastics for hydrogen production. *Catal. Today* https://doi.org/10.1016/j.cattod.2023.114084 (2023).

35. Yao, D., Yang, H., Chen, H. & Williams, P. T. Co-precipitation, impregnation and so-gel preparation of Ni catalysts for pyrolysis-catalytic steam reforming of waste plastics. *Appl. Catal. B* **239**, 565–577 (2018).

36. Zhang, J., Nakaya, Y., Shimizu, K. I. & Furukawa, S. Surface engineering of titania boosts electroassisted propane dehydrogenation at low temperature. *Angew. Chem. Int. Ed.* https://doi.org/10.1002/anie.202300744 (2023).

Acknowledgements

Author contributions

Competing interests

The authors declare no competing interests

Additional information

Supplementary information The online version contains supplementary material available at https://doi.org/10.1038/s41467-025-61051-2.

Correspondence and requests for materials should be addressed to Yongjun Gao, Tianfu Wang or Ding Ma.

Peer review information *Nature Communications* thanks Jinxing Chen and the other, anonymous, reviewer(s) for their contribution to the peer review of this work. A peer review file is available.

Reprints and permissions information is available at http://www.nature.com/reprints

Publisher's note Springer Nature remains neutral with regard to jurisdictional claims in published maps and institutional affiliations.